Research on the slamming effect of offshore platforms under extreme waves conditions

FU Li-ning [1,3], FENG Guo-qing [1,2], SUN Shi-li [1,2], LIU Peng-cheng [1,3], DU Shi-xin [1,3]

(1.College of Shipbuilding Engineering, Harbin Engineering University, Harbin, China

2.International Joint Laboratory of Naval Architecture and Offshore Technology between Harbin Engineering University and the University of Lisbon, 150001, Harbin, China.

3.HEU Qingdao Ship Science and Technology Co Ltd, Qingdao, China)

Abstract: With the booming of marine resources, it is vital to ensure the safety of offshore platforms under extreme waves. In the present study, the marine semi-submersible platform serves as the research target. The VOF method is employed for wave front tracking. In combination with the SST K-Omega model, the Navier-Stokes equation is solved to simulate the slamming effect under extreme waves. Mesh refinement is performed both on free surface and in fluid region around the platform. The wave conditions are selected following the DNV specification, and the rationality of the wave generation is proven by comparing the analytical wave height and the numerical wave height. Based on that, the slamming on fixed semi-submersible platform and freely moving semi-submersible platform under one-way regular wave is investigated. The deformation of the three dimensional free surface is simulated. The variation of impact pressure in time domain as well as its maximum magnitude are fully analyzed in every typical areas including the front and rear column, the lower deck and the front deck facing the wave flow. It is found that the slamming is most serious in the trapped area before the rear column and below the lower deck.

Key words: semi-submersible platform; regular wave; slamming effect; numerical simulation.

1 Introduction

The semi-submersible is considered as a major platform for exploiting marine resources. With the continuous development of marine resources, how to ensure the safety of semi-submersible platforms under extreme waves becomes increasingly important[1]. Wave slamming is a strong nonlinear

Contact author: Guoqing Feng, 15754516561@163.com

problem, which is a complicated coupling problem between the air, liquid and structure[2]. There exist three types of methods to study slamming problems. The first is the theoretical analysis, which usually simplifies the three-dimensional physical problem into a two-dimensional model which is solved based on the governing equations of fluid-structure and relevant theories subsequently[3]. The second is experimental research. The scale model, combined with a specific physical sensor, is built in line with a certain scale ratio, and the experimental research is conducted in the tank to analyze the relevant experimental phenomena[4]. The third one is numerical simulation, which selects the appropriate physical model, sets reasonable parameters, and solves related slamming problems using the current CFD software[5].

In this study, the extreme sea conditions are selected. The wave slamming effect of the semi-submersible platform is numerically simulated under the action of one-way incident wave. The slamming of waves on large-scale offshore structures can be generally simplified as that on platform decks and columns. By building a numerical tank model, the rationality of the wave is first verified. Subsequently, the wave slamming on a fixed platform is simulated without considering the structural response. Then, the platform is released with two degrees of freedom, that are pitch and heave motion activated by the incident wave. During the above slamming process, the emphasis is laid on the slamming effect on the platform's lower deck and column. Besides, the numerical simulation results are fully analyzed to draw relevant conclusions.

2 Theoretical basis

Marine structures are subjected to various forces during service in which wave load is considered here. After years of research by scholars, a mature theoretical basis has been developed for the simulation of the marine environment.

The mass conservation equation is written as:

$$\frac{\partial \rho}{\partial t}+\left[\frac{\partial(\rho u)}{\partial x}+\frac{\partial(\rho v)}{\partial y}+\frac{\partial(\rho w)}{\partial z}\right]=0 \tag{1}$$

The momentum conservation equations in directions of x, y and z have the following form:

$$\frac{\partial(\rho u)}{\partial t}+\frac{\partial(\rho u u)}{\partial x}+\frac{\partial(\rho u v)}{\partial y}+\frac{\partial(\rho u w)}{\partial z}=-\frac{\partial p}{\partial x}+\frac{\partial \tau_{xx}}{\partial x}+\frac{\partial \tau_{yx}}{\partial y}+\frac{\partial \tau_{zx}}{\partial z}+\rho f_x \tag{2}$$

$$\frac{\partial(\rho v)}{\partial t}+\frac{\partial(\rho v u)}{\partial x}+\frac{\partial(\rho v v)}{\partial y}+\frac{\partial(\rho v w)}{\partial z}=-\frac{\partial p}{\partial y}+\frac{\partial \tau_{xy}}{\partial x}+\frac{\partial \tau_{yy}}{\partial y}+\frac{\partial \tau_{zy}}{\partial z}+\rho f_y \tag{3}$$

$$\frac{\partial(\rho w)}{\partial t}+\frac{\partial(\rho w u)}{\partial x}+\frac{\partial(\rho w v)}{\partial y}+\frac{\partial(\rho w w)}{\partial z}=-\frac{\partial p}{\partial z}+\frac{\partial \tau_{xz}}{\partial x}+\frac{\partial \tau_{yz}}{\partial y}+\frac{\partial \tau_{zz}}{\partial z}+\rho f_z \tag{4}$$

where u, v, $w$denote the components of flow velocity in the x, y and z directions, respectively; τ_{xx},τ_{xy},τ_{xz}etc. refer to the components of the viscous stress; p is the pressure; f_x, $f_y$and $f_z$are components of the volume force[6].

For the boundary and initial conditions, the numerical wave tank here is considered as a transient problem of gas-liquid two-phase flow. At the initial moment, the water body is stationary. Thus, the velocity in the flow field is 0, and the pressure is consistent with the hydrostatic pressure distribution:

$$P = P_0 + \rho g h \tag{5}$$

The free surface is solved using the VOF (Volume of Fluid) method. The principle of the method is to trace the distortion of the free surface using the fluid and mesh volume ratio function $\alpha_q$in the grid unit.$\alpha_q$denotes a scalar representing the volume fraction of the qth phase fluid in the grid. $\alpha_q = 1$indicates that the grid cells are overall occupied by the specified phase fluid; $\alpha_q = 0$ means that no designated phase fluid exists in the grid unit; $0 < \alpha_q < 1$ reflects that there exists a part of the specified phase fluid in the grid unit. For the qth phase, the equation is written as:

$$\frac{\partial \alpha_q}{\partial t} + \frac{\partial (u_i \alpha_q)}{\partial x_i} = 0, (i = 1,2,3) \tag{6}$$

$$\sum_{q=0}^{1} \alpha_q = 1, (q = 0,1) \tag{7}$$

where $q = 0$denotes the air phase; $q = 1$is the aqueous phase[7].

3 Wave simulation

Following the *DNV* specifications, long term wave conditions are given as joint probabilities for significant wave height $H_s$and zero up-crossing period $T_z$or for H_s and spectrum peak period T_p. The most critical sea states for air gap of column stabilized units are the steep and high sea states. The steepness criterion is definedby a boundary$H_s = H_s(T_z)$given in terms of the average steepness of the sea state $S_s = 2\pi H_s / g T_z^2$ .The limiting values of S_s are taken as $S_s = 1/10$ for $T_z \leq 6\text{s}$ and $S_s = 1/15$ for$T_z \geq 12\text{s}$ and interpolatedlinearly between the boundaries. The steepness criterion curve is shown in Fig. 2.1. The design seastate should be searched along the steepness criterion curve for $H_s < H_{s,max} = 17.3\text{m}$[8].

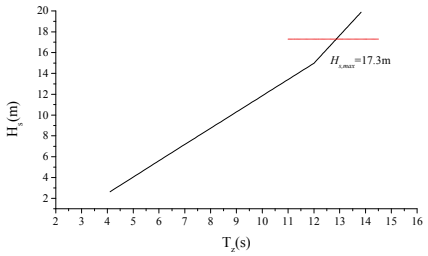

Fig. 1 (H_s, T_z) steepness criterion

Since irregular waves are largely uncertain, it is not conducive to systematic research. Accordingly, the Stokes fifth-order regular wave is applied here. The wave height of the sea state reaches 17.3m. According to the steep curve, the minimum wave period of this case is greater than 12s. Given this, the wave steepness is taken as 1/15, and the wave period is12.8s.

With the STAR CCM+ computing platform, in this example, a numerical tank is established with a length of 600m, a width of 300m, a water depth of 250m and an air layer height of 150m. The N-S equation is solved using a two-dimensional separation implicit transient method; the changes in free surface are monitored in accordance with VOF theory; the wave field information near the wall area is calculated using the wall function method; the discrete method of the center difference format is selected to discretely solve the governing equation of the wave field. At the beginning of the submission of the calculation, the first-order up-style can be selected for initial calculation and analysis, which is easier to converge. When the calculation of the wave field is stable, it can be transformed into a second-order up-style. The PISO pressure and velocity coupling method is adopted for the iterative calculation of discrete forms of momentum equations and continuous equations[9].

In terms of grid convergence verification, the accuracy of wave simulation varies with mesh density. Grid convergence study is required to determin the optimal mesh density. According to experience, at least 20 grids should be set in the unit wave height direction, and at least 80 grids should be set in the unit wavelength direction[10]. Therefore, 3 grids A, B and C are verified. In the unit wave height direction, Grid A contains 20 grids, Grid B contains 28 grids and Grid C includes 35 grids.

Table1 Grid size and quantity

	Min size in the X	Min size in the Y	Min size in the Z	Total number
A	0.875m	3.500m	3.500m	525192
B	0.625m	2.500m	2.500m	1267200
C	0.500m	2.000m	2.000m	2565736

For comparing the difference between the theoretical and the actual wave height, a virtual wave height instrument is arranged in the numerical tank to verify the accuracy of the wave. The position of the wave height instrument from the speed entrance is listed in Table 2.

Table2 Position of the wave height instrument

Point	1/2	3/4	5/6	7/8	9/10	11/12	13/14
Distance/m	1	100	200	300	400	500	599

It is noteworthy that this example refers to the Convective Courant Number as the reference standard for calculation to ensure the stable calculation of the flow field during the wave-making process. Moreover, the Convective Courant Number is ensured to be less than 0.1[11].

After calculation, the theoretical and actual values of each measuring point are obtained, and the effects of different mesh densities on the wave precision are selected by measuring point 6 and measuring point 8. The results are shown in Fig. 2 and Fig. 3, respectively.

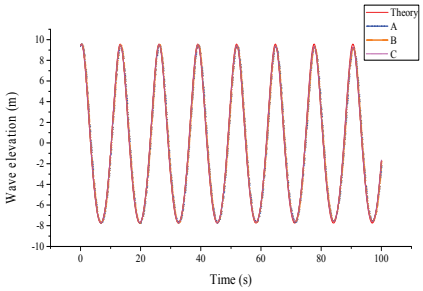

Fig. 2 measuring Point 6

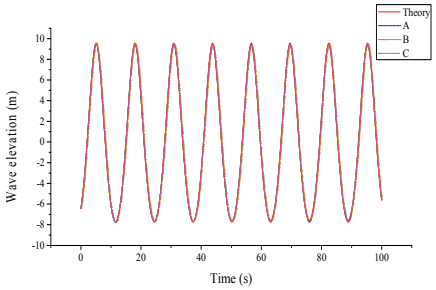

Fig. 3 measuring point 8

By comparing the theoretical wave shape with the actual wave shape at different grid densities, the accuracy in three cases meets requirements.

The detailed error analysis is conducted to clarify the effect of grid density in the wave simulation. The following is to briefly describe the error analysis method, and two methods are considered in this study. The first is the average error and the second is the maximum error.

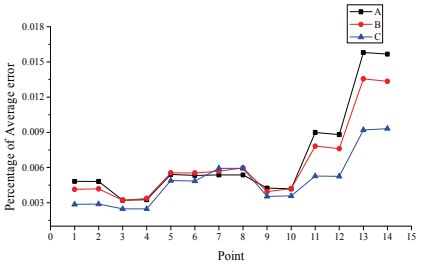

Fig.4 The percentage of average error

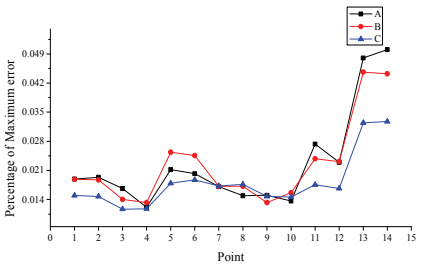

Fig. 5 The percentage of maximum error

It can be seen from the Fig.4 and Fig.5 that the accuracy of wave simulation under the three grid densities is very high, and all meet the requirements. Considering the limitation of computing resources and time, grid B is employed in the subsequent calculation of semi-submersible platform wave slamming.

4 Platform wave slamming simulation

4.1 The platform and main particulars

Based on the ensured wave accuracy, this study explores the slamming effect of extreme waves on semi-submersible platforms. The platform model is shown in Fig.6. The main scale parameters are shown in Table 3.

Table3 The main scale of Platform

Deck size	97.75m×87m×8.8m
Column size	19.25m×18.5m×25m
Attached body size	123.6m×20.5m×11.5m
Draught Depth	23m
Hydrostatic air gap	13.5m

Since the semi-submersible platform is affected by waves, there exists a coupling divided into one-way coupling and two-way coupling between the structure and the wave field in the marine engineering. One-way coupling considers the effect of fluid on structure, solving structural stress field must be based on solving flow field. Structural stress field analysis should be dependent on flow field analysis results, yet it does not affect flow field analysis. In two-way coupling, the analysis of the stress field in turn affects the state of the flow field. In this chapter, the one-way coupling example is first analyzed, and then the two-way coupling is explored[12].

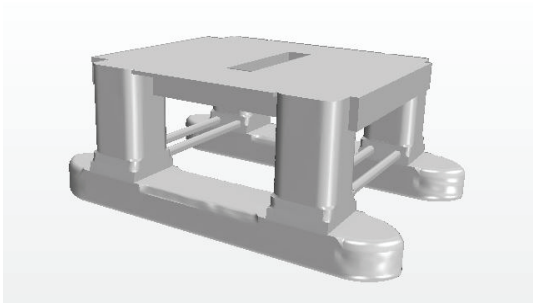

Fig. 6 Semi-submersible platform model

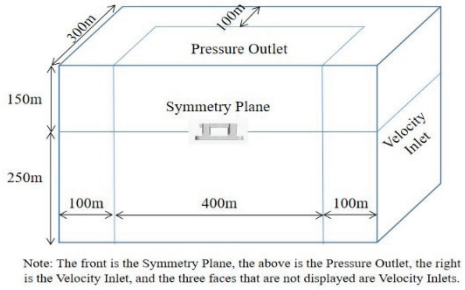

Fig. 7 The layout of computational domain

4.2 Wave slamming on fixed platform

For computational domain setting, given the symmetry of the platform and the consumption of computing resources, the example employs semi-domain calculation. The computational domain is 600m long, 300m wide and 250m deep, with air layer of 150m. For boundary conditions, the surface above the platform is set to pressure outlet. The center plane of the platform is set to symmetry plane, and the rest is set to velocity inlet, as shown in Fig.7. The wave conditions use the extreme waves of Section 2, with a wave height of 17.3 m and a wave period of 12.8 s.

The three-dimensional unsteady implicit method is adopted where the fluid is consumed to be incompressible. The governing equation is solved based on the finite volume method (FVM) by using the “collocated grid” to store the flow field parameters. The pressure and velocity are stored in the center of the control unit. The SST K-Omega turbulence model is employed. Since this problem belongs to the non-steadyinteraction between wave and structure in time domain, the pressure-velocity coupling method (PISO) is used to solve the discrete form of the momentum equation iteratively,

yielding the convergent results of pressure and velocity. The VOF method is applied in the free surface treatment. EOM is employed and the wave forcing length is set to 100m. In the present case, the wave period is chosen as 12.8s , and considering that wave slamming is transient, the time step is set to 0.01s.

Mesh refinement is performed on free surface with at least 28 grids in one wave height and also required for the fluid around the platform as shown in Fig.8. The measuring points are placed on the front and rear columns, the lower deck and the deck facing the wave flow. The waterline is coincident with the 3rd line of measuring points as shown in Figs.9-11[13].

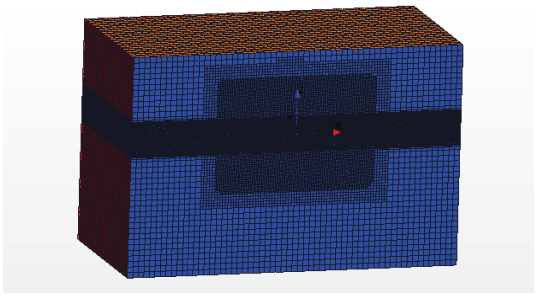

Fig. 8 Mesh of computational domain

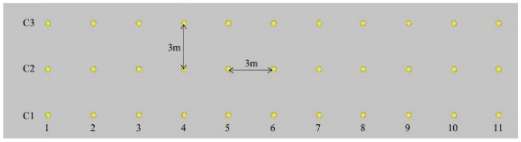

Fig. 9 Deck facing the wave flow

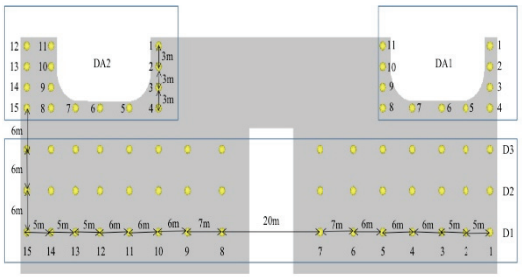

Fig.10 Lower deck

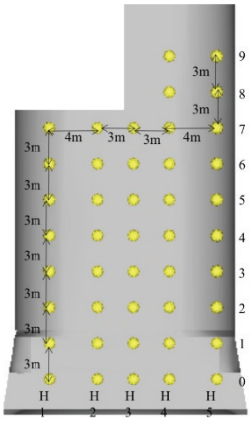

Fig.11 Front and rear column

By observing the calculation results, it was found that the wave slamming near the area connecting the rear column and the lower deck is very serious. When the wave propagates to that area, the space is confined to a small space, the velocity of the fluid particles will increase, the disturbed wave becomes larger, and thus the wave crashes on the rear column which leads to large impact pressure there. The change of pressures with time on measuring point DA2-2 and H2-7 is respectively shown in Figs 12-13.

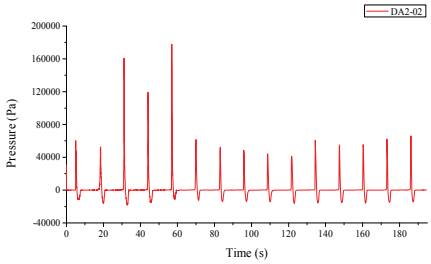

Fig.12 Pressure at measuring point DA2-2

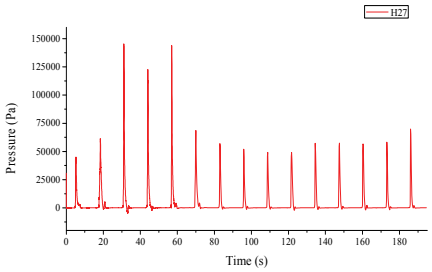

Fig.13 Pressure at measuring point H2-7

The maximum value is picked from the above time history curves of the pressure and then plotted in Figs 14–18 for the measuring points in different regions.

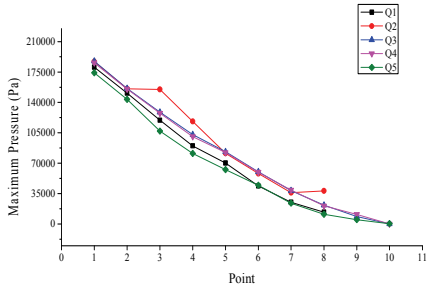

Fig.14 Max pressure at points of front column

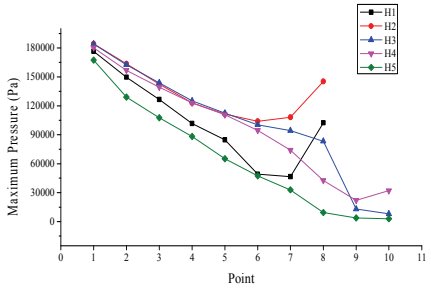

Fig.15 Max pressure at points of rear column

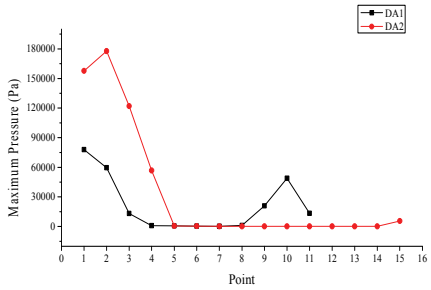

Fig.16 Max pressure at points of lower deck DA

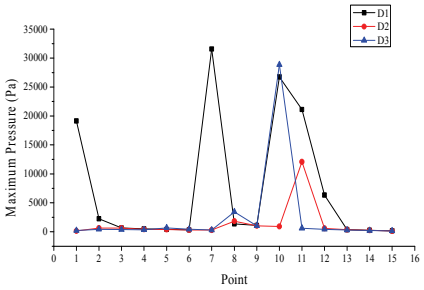

Fig.17 Max pressure at points of lower deck D

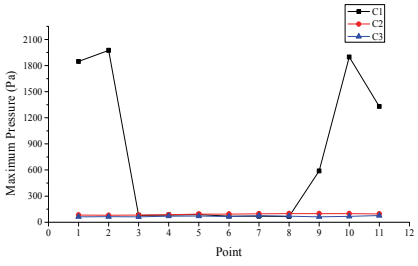

Fig.18 Max pressure at points of deck facing wave flow

The total simulation time is 15 wave periods, which is nearly 192s. For the front column, the maximum slamming pressure increases when the measuring point is placed lower. For the rear column, the slamming phenomenon is similar to that on the front column, yet there is still differences. Since the top of the rear column is confined by the lower deck, the fluid is found to strenuously move in a limited space, creating a small air gap and even a negative air gap. In turn, the local velocity of the wave suddenly increases, causing a severe slamming phenomenon. It should be noticed that sometimes the slamming pressure on the high positioned measuring points is even larger than that on the low positioned measuring points. For instance, the minimum pressure usually appears on the highest positioned measuring points H-8. But an exception is that the slamming pressure on the measuring points H1-8 and H2-8 is much larger than the minimum value within the same line, and the minimum value stays at about H1-6 and H2-6.

For the lower deck denoted by DA as shown in Fig.19, the slamming pressure on the measuring points DA2-1, DA2-2, DA2-3, DA2-4 is relatively large, which is noteworthy. This is because these measuring points not only face the wave, but also are placed in trapped area within 4 columns. The back-wave surfaces numbered 9, 10 and 11 are blocked by the columns, resulting in the slamming effect almost negligible. The rest measuring points on the lower deck have some distance from the 4 columns and the disturbed wave there is relatively smaller, and thus the slamming rarely occurs due to the large air gap. There is no slamming on the deck marked by C facing the wave flow, as it is high positioned and away from the wave surface.

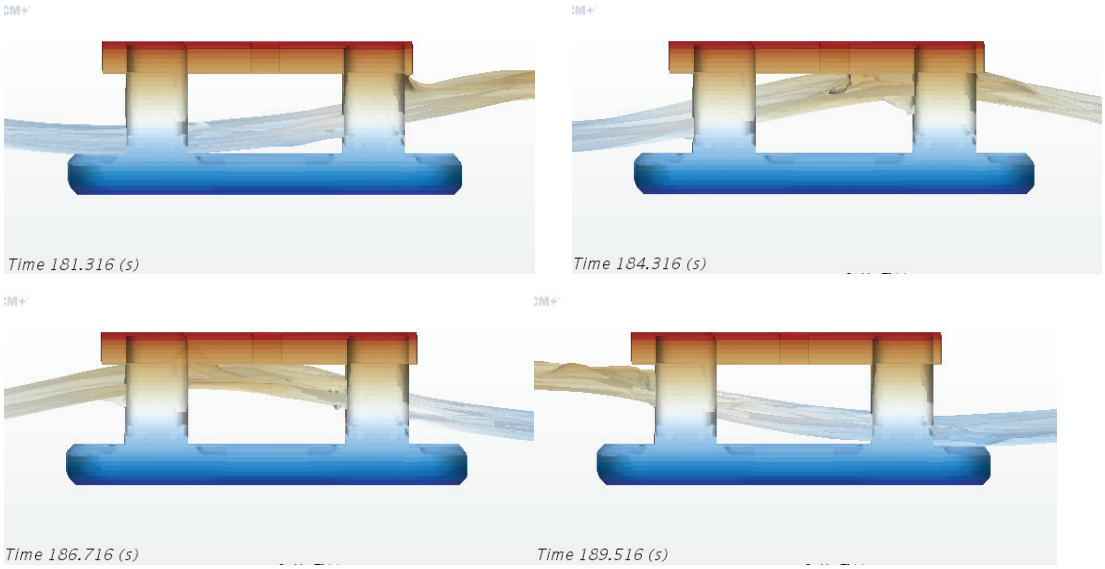

Fig.19 Wave surface at different times

4.3 Wave slamming on the platform in pitch and heave motions

The fixed platform is studied in Section 3.2. Based on that, the moving platform in wave is investigated in the present section. The two degrees of freedoms are released, namely pitch and heave. The parameter setting of the platform motion is briefly described[14].

Table4 The parameters of the moving platform

Body Mass	3.68E7 kg
Body Motion Option	Free Motion
∟	Z motion / Y Rotation
Center of Mass	$[-1.11\mathrm{m}, 0.0\mathrm{m}, -0.37\mathrm{m}]$
Moment of Inertia	$[7.675E9, 8.525E9, 1.3055E10]\mathrm{kg}\cdot\mathrm{m}^2$
Orientation	Laboratory

Overlapping meshes are applied here, and the size of the nested mesh is consistent with the background mesh in the three directions of X, Y, and Z. The initial mesh is illustrated in Fig. 3.15. After the calculation, the mesh changes and are shown in Fig. 3.16.

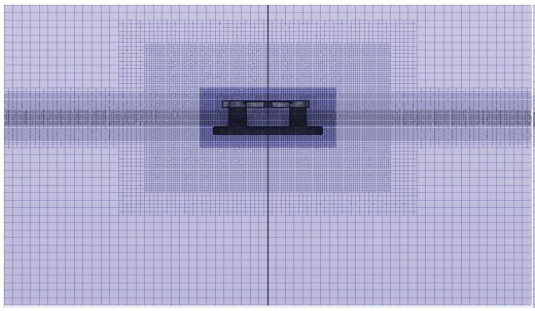

Fig.20 Initial grid

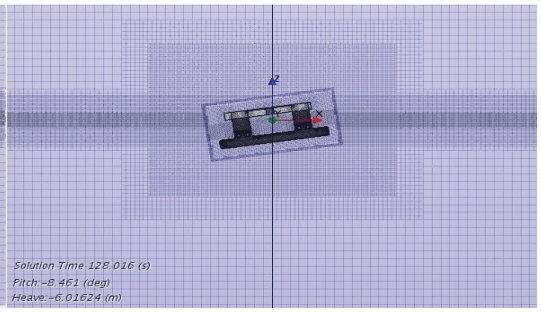

Fig.21 Grid after a while

The total simulation time is 10 wave periods, which is nearly 128s. The time history curve of heave and pitch under the action of the wave is obtained. They are respectively shown in Figs 22-23. It is shown that heave and pitch exhibit the similar periodicity to waves. In the initial stage of calculation, the moving amplitude is large and not regular due to the instability of the flow field. Gradually, heave and pitch becomes stabilized. In this case, only two degrees of freedoms are released, and the constraints are not considered. The largest pitch angle reached 20^{o}, which exceeds the standard requirements [15], which requires special attention.

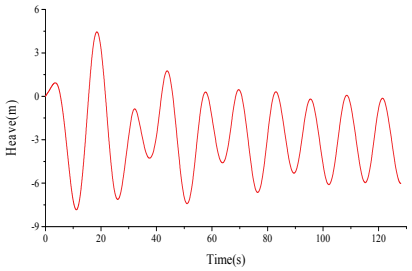

Fig.22 Heave

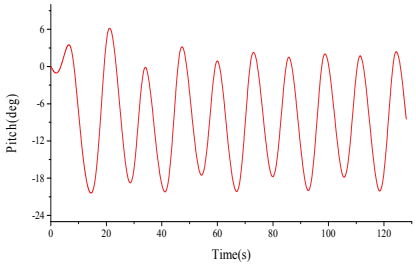

Fig.23 Pitch

Figs 24–28 show the maximum impact pressure in different regions. The overall variation trend for a moving platform case is similar to that for the fixed one. For example, the interaction area between the lower deck and the column is also most dangerous here.

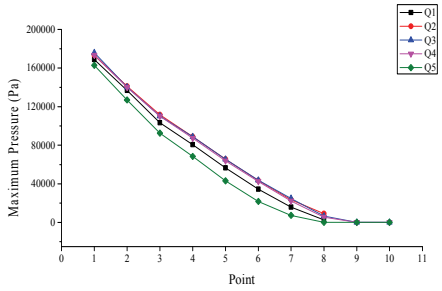

Fig.24 Max pressure at points of front column

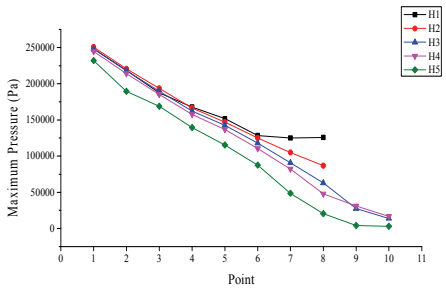

Fig.25 Max pressure at points of rear column

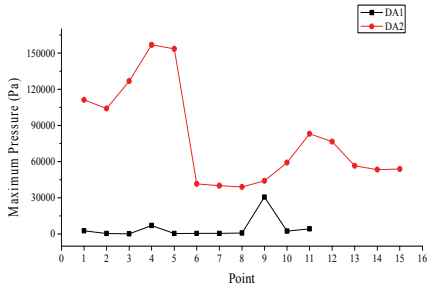

Fig. 26 Max pressure at points of lower deck DA

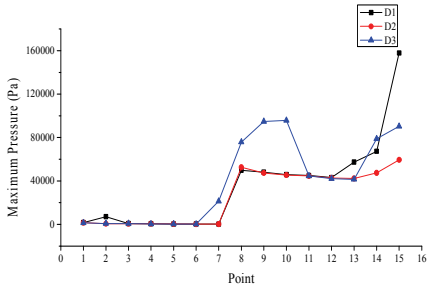

Fig.27 Max pressure at points of lower deck D

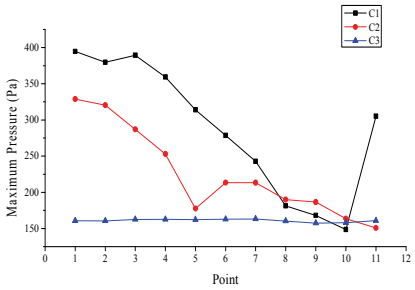

Fig.28 Max pressure at points of deck facing wave flow

The initial air gap between the lower deck and the undisturbed wave surface is 13.5 meters, and the wave height is 17.3 meters. The wave climbs along the column and crashes the lower deck, thereby generating a large slamming pressure. In such a case, the slamming pressure only affects the local structure without affecting the overall strength of the platform; the wave impact platform column can be considered as a huge fluid micelle against the column, thereby affecting the overall strength of the platform.

5 Conclusions

The problem of incident waves impacting on a platform is simulated. The incident wave is convergent with respect to mesh size and conforms with the analytical solution. The simulation covers slamming on a fixed platform and a freely moving one. At least 20 grids in the wave height direction is meshed to ensure the accuracy. The conclusions are drawn as follows:

The wave slamming near the area before the rear column and below the lower deck is very serious. When the wave propagates to that area, the space is confined to a small space, the velocity of the fluid particles will increase, the disturbed wave becomes larger, and thus the wave crashes on that region which leads to large impact pressure there. The maximum slamming pressure overall increases when the measuring point is placed lower both for front and rear column. But there may be an exception that the slamming pressure on the high positioned measuring points is larger than that on the low positioned points. The back-wave surface is blocked by the columns, resulting in the slamming effect almost negligible. For the measuring points on lower deck that have some distance from the 4 columns, the disturbed wave there is relatively smaller, and thus the slamming rarely occurs due to the large air gap. In the case of moving platform, only two degrees of freedoms are released, and the constraints are not considered. The largest pitch angle reached 20^{o}, which exceeds the standard requirements, which requires special attention.

ACKNOWLEDGEMENTS

This work is financially supported by the innovation project of the seventh generation of ultra-deep water drilling platform (ship). This support is gratefully acknowledged. And this work is also supported by the National Natural Science Foundation of China (Grant No. 51679045). The authors would also like to thank the editor and anonymous reviewers for their comments which have led to a much improved paper.

REFERENCES

1 Ma Z. Wave slamming and its interaction effects with deepwater semi-submersible platforms under extreme wave conditions, 2014,10–16. PhD these, (in Chinese)

2 Nielsen F. G. Comparative study on air gap under floating platforms and run-up along platform columns, Marine Structures, 2003, 16(2): 97–134.

3 Sun S.L., Sun S.Y., Wu G.X. A three dimensional infinite wedge shaped solid block sliding into water along an inclined beach, Journal of Fluids and Structures, 2016, 669: 447–461.

4 Dong C.R., Sun S.L., Song H.X., et al. Numerical and experimental study on the impact between a free falling wedge and water. International Journal of Naval Architecture and Ocean Engineering, 2019, 11(1): 233–243.

5 Hu J., Lun Z.Q., Kan X.Y., et al. Numerical Simulation on Interface Evolution and impact of Flooding Flow. Shock and Vibration, 2015, 794069:1–12.

6 Dong Z., Zhan J.M. Numerical modeling ofwave evolution and run-up in shallow water, Journalof Hydrodynamics, 2009, 21(6):731-738.

7 Yang Q.X., Feng G.Q., The numerical analysis of the wave slamming load on deep-water platforms. Editorial Board of Ship Mechanics, China Ship Science Research Center: Editorial Department of Ship Mechanics, China Ship Science Research Center, 2017: 1 - 12. (in Chinese)

8 DET NORSKE VERITAS. DNVGL–OTG–13, Prediction of air gap for column stabilised units. 2016–09.

9 Shan T.B., Lu H.N., Yang J.M., et alNumerical experimental and full-scaled investigation on the current generation system of the new deep water offshore basin. Proceedings of the ASME 29th international conference on ocean, offshore and arctic engineering, 2010, 4:349–355.

10 Alexandre N.S. Experimental evaluation of the dynamic air gap ofa large-volume semi-submersible platform. 25th International Conference on Offshore Mechanics and Arctic Engineering(OMAE 2006). Hamburg, Germany. 2006, 1–7.

11 Shan T.B. Research on the mechanism of wave run-up and the key characteristics of air-gap response of semi-submersible, 2013, 53–59. PhD these, (in Chinese).

12 Zhu H. Studies on the motion performance of a semi-submersible platform and the heave motion damping system using moveable heave-plate, 2011, 80–94. PhD these, (in Chinese).
13 Zhou S.L., Nie W., Bai Y. Study on the Design of Mooring System for Deepwater Semi-submersible Platform, Journal of Ship Mechanics, 2010, 14(05): 495–502. (in Chinese).
14 Kazemi S., Incecik A. Theoretical and experimentalanalysis of air gap response and wave-on-deck impactof floating offshore structures, Proceedings of the26th International Conference on Offshore Mechanicsand Arctic Engineering(OMAE2007), San Diego, California,USA, 2007, 297–304.
15 Liu K., Ou J.P. A novel tuned heave plate system for heave motion suppression and energy harvesting on semi-submersible platforms. Science China(Technological Sciences), 2016, (06): 897–912.